

N89-21746

1988

NASA/ASEE SUMMER FACULTY RESEARCH FELLOWSHIP PROGRAM

MARSHALL SPACE FLIGHT CENTER  
THE UNIVERSITY OF ALABAMA

THE SIMULATION OF THE ALTERNATE TURBOPUMP DEVELOPMENT  
HIGH PRESSURE OXYGEN AND FUEL TURBOPUMPS FOR THE  
SPACE SHUTTLE MAIN ENGINE USING THE SHABERTH COMPUTER PROGRAM

Prepared by: Gary H. McDonald, Ph.D, P.E.

Academic Rank: Assistant Professor

University and Department: The University of Tennessee  
at Chattanooga  
Mechanical Engineering --  
Mechanics

NASA/MSFC:

Laboratory: Propulsion  
Division: Component Development  
Branch: Turbomachinery and  
Combustion Devices

NASA Colleague: Henry P. Stinson

Date: August 19, 1988

Contract No.: NGT 01-002-099  
The University of Alabama

THE SIMULATION OF THE ALTERNATE TURBOPUMP  
DEVELOPMENT HIGH PRESSURE OXYGEN AND FUEL  
TURBOPUMPS FOR THE SPACE SHUTTLE MAIN ENGINE  
USING THE SHABERTH COMPUTER PROGRAM

by

Gary H. McDonald  
Assistant Professor of Engineering  
in Mechanical--Mechanics  
The University of Tennessee at  
Chattanooga  
Chattanooga, Tennessee

ABSTRACT

The space shuttle main engine (SSME) is basically comprised of a combustion chamber and nozzle, high and low pressure oxygen turbopumps and high and low pressure fuel turbopumps. In the current configuration, the high pressure fuel (HPFTP) and high pressure oxygen turbopumps (HPOTP) have experienced a history of ball bearing wear. The wear problem can be attributed to numerous factors including the hydrodynamic axial and radial loads caused by the flow of liquid oxygen and liquid hydrogen through the turbopump's impellers and turbine. Also, friction effects between the rolling elements, races, and cage can create thermally induced bearing geometry changes. If the frictional heat generation becomes greater than the available coolant capacity and if the hydrodynamic loads become excessive, then, then thermal effects and loading can contribute to eventual bearing failure. To alleviate some of the current configuration problems, Pratt and Whitney has proposed the alternate turbopump development (ATD). However, the ATD HPOTP and HPFTP are constrained to operate interchangeably with the current turbopumps, thus, the operation conditions must be similar. The ATD configuration features a major change in bearings used to support the integrated shaft, impeller and turbine system. A single ball and single roller bearing will replace the pump-end and turbine end duplex ball bearings.

In this study, the SHABERTH (Shaft-Bearing-Thermal) computer code was used to model the ATD HPOTP and ATD HPFTP configurations. A two-bearing model was used to simulate the HPOTP and HPFTP bearings and shaft geometry. From SHABERTH, a comparison of bearing reaction loads, frictional heat generation rates, and Hertz contact stresses will be attempted with Pratt and Whitney's analysis at the 109% and 65% power levels.

### ACKNOWLEDGEMENTS

Several individuals have provided important contributions in this author's NASA/ASEE fellowship project. I would first thank Dr. L. Michael Freeman, director of the MSFC NASA/ASEE fellowship program and Ms. Ernestine Cothran, director of MSFC university relations, for their diligent efforts in the organization of seminars, tours, and the general administration of this worthwhile program. I thank them for the opportunity to again participate in this program for a second summer.

I would especially like to thank my colleague Mr. Henry P. Stinson who was valuable in formulating this year's project and providing the necessary technical assistance. A special appreciation is extended to Mr. Dale Blount of NASA/MSFC and Mr. John Price and Mr. Yul Eren of Pratt and Whitney who provided the technical information to model the alternate turbopump development design.

Also, a grateful appreciation is extended to Mr. Joe Cody and Mr. Dave Marty of SRS/System Division who provided information concerning the ATD ball bearing for the program's input. Dave loaded both the SHABERTH code and a CLIST execution program on the IBM EADS for the author. Also, an example input file was loaded for the latest version of SHABERTH code which was utilized in this project. Also, Dave supplied helpful information on the use of IBM-Engineering Analysis and Data System (EADS). A special appreciation must be expressed to Ms. Julie Bomar, UTC-School of Engineering, who diligently typed this report.

I finally express my gratitude to Mr. Loren Gross and all the members of the Turbomachinery and Combustion Devices Branch for their technical guidance, assistance, and encouragement that has made my two summers at MSFC an enjoyable and productive experience.

ORIGINAL PAGE IS  
OF POOR QUALITY

INTRODUCTION

The space shuttle main engine (SSME) is basically comprised of a combustion chamber, nozzle, high and low pressure fuel and oxygen turbopumps. In the current configuration, the high pressure fuel and oxygen turbopumps (HPFTP and HPOTP) have had a history of ball bearing wear. This wear has contributed to numerous factors including hydrodynamic axial and radial loads caused by the flow of liquid hydrogen (LH2) and oxygen (LOX) through the turbopump's impellers and turbines. Also, wear caused by friction effects creates thermally induced bearing geometry changes. Pratt and Whitney Aircraft [8] has been contracted to develop an alternate design for the high pressure oxygen and fuel turbopumps. This alternate turbopump development (ATD) will hopefully alleviate the bearing wear problems of the current design. However, the ATD turbopumps are constrained to operate interchangeably with current turbopump configurations; thus, the ATD must have the same operating conditions to generate the power levels of the current SSME turbopumps. Since the ATD is in the development phase of design, the first step in proving the feasibility of the proposed changes is analytical. Once an analytical basis is established, then the construction and instrumentation of the bearing testers is completed to provide the necessary test data for rating the bearing's performance. The final phase will be the construction and testing of high pressure fuel and oxygen turbopumps. The testing of the turbopumps in an engine system will generate the necessary database to confirm the ATD design for flight standards.

In the analytical phase, one tool in the prediction of bearing behavior is the use of the SHABERTH (Shaft-Bearing-Thermal) computer program. This program, originally developed by SKF Industries, has been greatly modified by SRS Technologies/System Division of Huntsville, Alabama, to model HPFTP and HPOTP for NASA Marshall Space Flight Center (MSFC). SHABERTH input data necessary for the program's execution is a collection of information concerning the bearing's and shaft's geometry and material properties, the location and magnitude of the loads applied to the shaft and the initial thermal environment of the bearings. The collection of input data was performed in this study for both the ATD high pressure fuel and oxygen turbopump configurations. From this given information, SHABERTH will calculate frictional heat generation, bearing Hertzian contact stresses, bearing clearance changes and bearing reaction loads. These are only a sample of SHABERTH's output results, but will be the chosen results to indicate the bearing's performance in this study.

For sample input and output listings, references [4,5] are useful. These references are the user manuals for the SHABERTH program.

### ATD Design

The ATD high pressure oxygen turbopump (HPOTP) configuration is shown schematically in Figure 1. The turbopump consists of the same major components as the current configuration. These components are a preburner impeller, main impeller, and turbine disk with blades which are integrated into a system by a common hollow shaft. The main differences in the ATD HPOTP design are the choice of bearings to support the shaft. Currently, a duplex pair of 45 mm bore ball bearings support the pump end, whereas a duplex pair of 57 mm bore ball bearings support the turbine end of the HPOTP. The 45 mm bore pump end ball bearings have been replaced with a single 60 mm bore ball bearing. On the turbine end, the 57 mm bore ball bearings have been replaced by a single 73 mm bore cylindrical roller bearing.

Also, shown in Figure 1 on the turbine end, a small thrust ball bearing exists. Its purpose is to react any transient unbalance axial load toward the turbine. This thrust ball bearing is to only carry transient axial load since cylindrical roller bearings are, by design, radial load carriers. Unfortunately, this thrust bearing is not included in this simulation. This exclusion is due to insufficient information concerning the thrust bearing's geometry at this time. These axial loads are only significant in the start-up or shut-down of the engines. Since a 109% full power level has been chosen to be simulated in this study, these axial loads will not be considered. So, the exclusion of the thrust bearing should not significantly affect the results of this simulation.

Another difference in the ATD HPOTP is the location of the interpropellant seal package. The labyrinth seals are now between the roller bearing and the main impeller. This allows the roller and thrust ball bearing to be operated in a liquid hydrogen (LH2) environment. Whereas, the HPOTP ball bearing will operate in a liquid oxygen (LOX) in environment.

The ATD high pressure fuel turbopump (HPFTP) configuration is shown schematically in Figure 2. Again, this turbopump consists of the same major components as the current configuration. The HPFTP consists of first, second, and third stage impellers and a turbine blades and disk that are integrated onto a hollow shaft. The ATD HPFTP replaces the 45 mm bore duplex pair pump end ball bearings with a single 63 mm ball bearing and the 45 mm bore duplex pair turbine end ball bearings with a single 73mm bore cylindrical

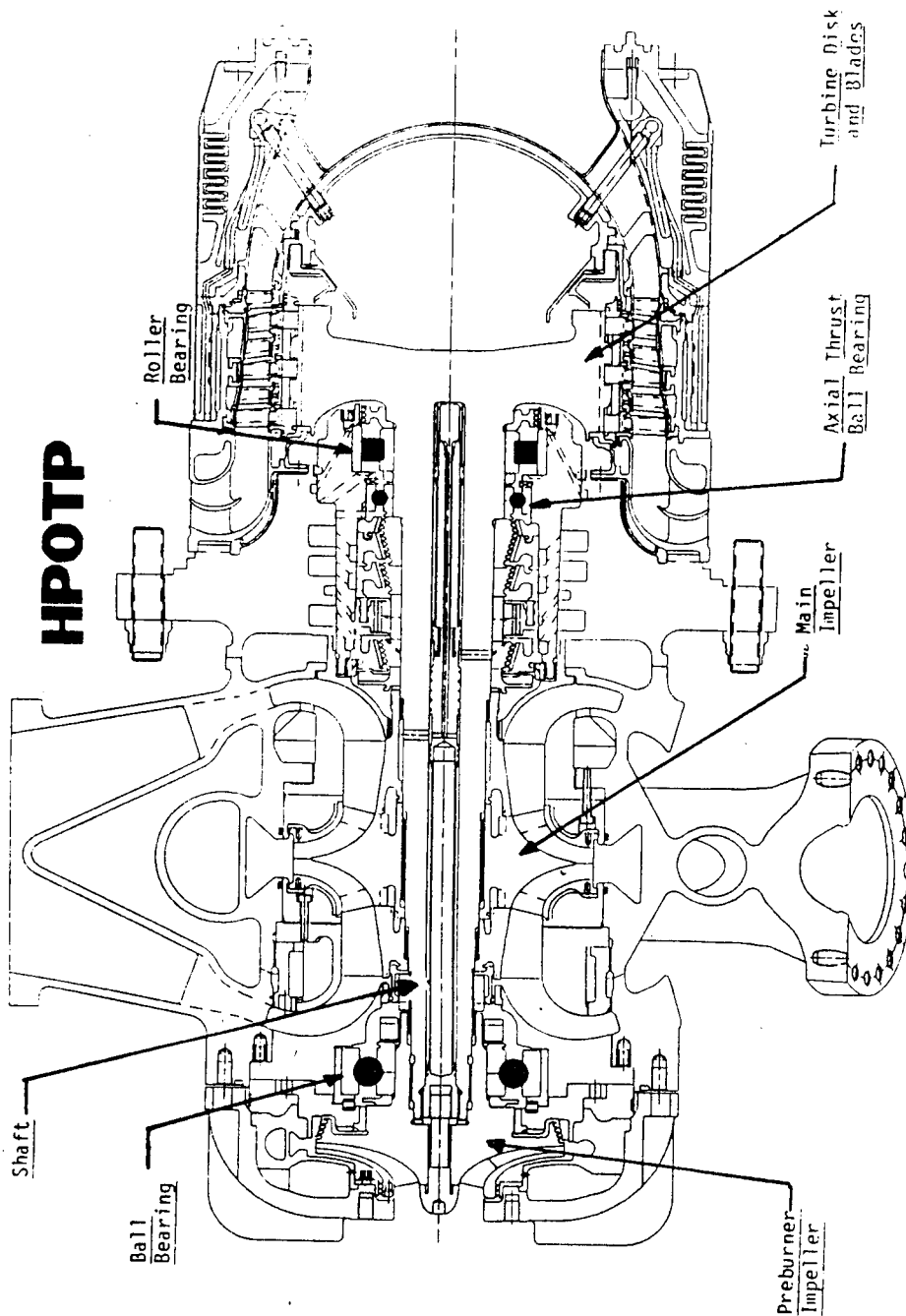


Figure 1: Schematic of the High Pressure Oxygen Turbopump (HPOTP)

# HPFTP

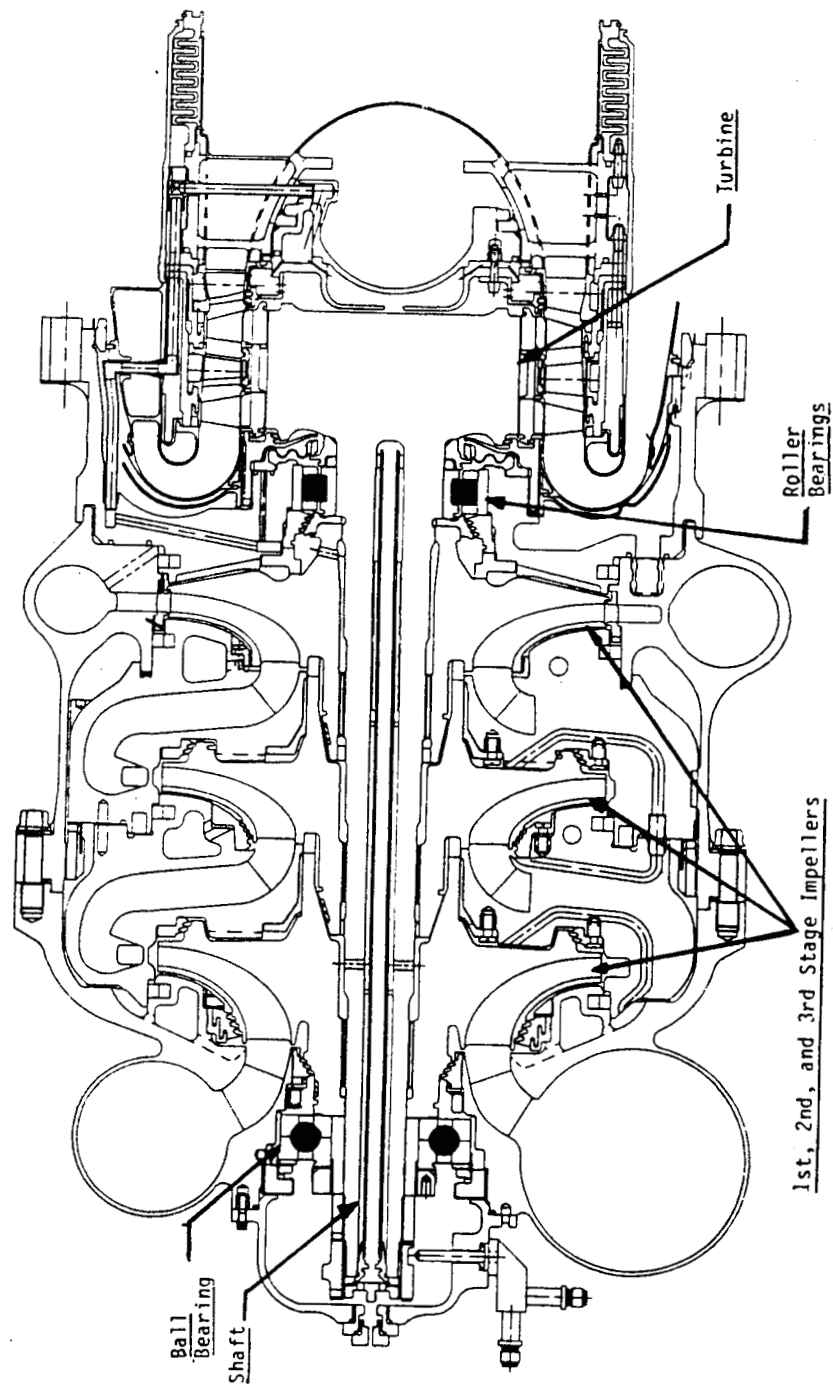


Figure 2: Schematic of High Pressure Fuel Turbopump (HPFTP)

roller bearing. In the HPFTP, no thrust ball bearing is necessary since there exists a balance piston and rub-stops to control any axial movement. Thus, the roller bearing should be reacting to only radial loads. Both the ball and roller bearings will be operating in the liquid hydrogen (LH2) fuel environment.

#### OBJECTIVES

The purpose of this study is to model the ATD HPOTP and HPFTP configurations using the SHABERTH computer program. Using the results of these simulations, a comparison will be attempted to Pratt and Whitney's predicted values for bearing reaction loads, frictional heat generation and Hertzian contact stresses. Pratt and Whitney performed one bearing models for both the HPFTP and HPOTP ball and roller bearings using SHABERTH. From SHABERTH, they predicted the frictional heat generation, while from the A.B. Jones bearing program, they obtained values for Hertzian contact stress. Therefore, the objectives of this project were

1. To collect radial hydrodynamic load information representing the effects of the major components of the HPOTP and HPFTP for 109% power level and the 65% power level.
2. To create input data files representing the ball and roller bearing geometry and material properties, the shaft size, initial temperatures at 13 locations on the bearing due to coolant flow, coefficients of friction, axial preload for the bearings and the magnitude and location of the hydrodynamic radial loads along the shaft.
3. To attempt a comparison of reaction bearing loads, frictional heat generation and Hertzian contact stress of the two-bearing HPOTP and HPFTP SHABERTH models to Pratt and Whitney or SRS Technologies results.

#### SHABERTH Computer Model

SHABERTH performs a thermo-mechanical simulation of a load support system consisting of a flexible shaft supported by up to five rolling element bearings. The shaft can be hollow or solid and of arbitrary geometry. Any combination of ball, cylindrical, or tapered roller bearings can be used to support the shaft. The applied loading can consist of point or distributed moments, point or distributed forces and shaft misalignments. Bearing operating clearance is determined as a function of shaft and housing fits. A lumped



mass thermal model allows calculation of steady state or time transient system temperatures considering free and forced convection, conduction, radiation and mass transport heat transfer. The purpose of this program is to provide a tool in which the shaft bearing system performance characteristics can be determined as functions of system temperatures. These system temperatures may be either steady state or transient. The bearing theory used in SHABERTH is found in a reference by Harris [1]. Other bearing theory sources are found in references [2,3]. For a complete discussion concerning SHABERTH's structure, references [4,5] are program's first and second generation user manuals. These manuals provide the user with examples of input format tables and output listings for various cases.

The ball bearing information for both the ATD HPOTP and HPFTP was supplied by SRS Technologies/System Division of Huntsville, Alabama. The ATD HPOTP and HPFTP ball bearing's inner race, outer race and bearing material are made from 440C steel. Each ball consists of 11 rolling elements with a ball diameter of 20.6 mm (0.81 in.). The bearing bore diameter is 60 mm (2.36 in.), the bearing outer diameter of 130 mm (5.12 in.) and the bearing inner and outer ring widths of 30.6 mm (1.2 in.). The HPOTP and HPFTP ball bearings have a diametrical clearance of 0.1698 mm (0.00668 in.) and a pitch diameter of 100 mm (3.94 in.). A prediction of the ball-race dry coefficient of friction is 0.25. The dry coefficient of friction between the ball and cage is predicted to be 0.2. Initially, the ball bearing in the HPOTP will be cooled with liquid oxygen (LOX) at -145°C (-220°F) while the HPFTP ball bearing will experience a -202°C (-331.6°F) liquid hydrogen (LH2) coolant.

The ATD HPOTP and HPFTP roller bearings have inner races made of 440C (AMS 5618) and outer races made of AISI 9310 (AMS 6265). The outer race material was chosen to reduce cracking possibilities which occurred when 440C was used for the outer race material. Both roller bearings contain 14 rolling elements. The HPOTP roller bearing has a roller length of 15 mm (0.59 in.) and roller diameter of 15 mm (0.59 in.). Its roller crown radius is 695.9 mm (27.4") and its roller flat length is 7.62 mm (0.3 in.). The HPOTP roller bearing has a bore diameter of 73 mm (2.87 in.), a bearing outer diameter of 133 mm (5.24 in.), an inner-ring width of 28.64 mm (1.1275 in.) and an outer ring width of 30.54 mm (1.2024 in.). The HPOTP roller diametrical clearance is -0.0381 mm (-0.0015 in.). The HPFTP roller bearing has a length of 17 mm (0.669 in.) and a roller diameter of 17 mm (0.669 in.). Its roller crown radius is 632.5 mm (24.9 in.) and its roller flat length is 8.89 mm (0.35 in.). The HPFTP roller bearing also has a bore diameter of 73 mm (2.87 in.)

ORIGINAL PAGE IS  
OF POOR QUALITY

but a bearing outer diameter of 127 mm (5 in.), an inner ring width of 34.61 mm (1.3625 in.) and an outer ring width of 32.54 mm (1.281 in.). The HPFTP roller diametrical clearance is -0.0685 mm (-0.0027 in.) and a pitch diameter of 103 mm (4.06 in.). A prediction of the roller-race, roller-cage, and flange-end dry coefficient of friction for the HPOTP and HPFTP roller bearings is 0.1. Initially, the HPOTP roller bearing will be cooled with liquid hydrogen (LH2) at -118°C (-180.4°F); whereas, the HPFTP roller bearing will experience cooling from liquid hydrogen at -202°C (-331.6°F).

At the 109% full-power level, the HPOTP shaft speed or bearing inner ring speed is predicted to be 25,977 rpm. In contrast, the 65% power level for the HPOTP is approximately 17,000 rpm. For the HPFTP, its 109% power level shaft speed is 38,482 rpm while at 65% power level, its shaft speed is 28,500 rpm.

The dimensions for the inner and outer shaft diameters and the x-direction locations of these diameter changes were determined by measuring the distances from a blue line drawing of the ATD HPOTP and HPFTP. A scale factor of 1.05 was used to magnify the measured distances to their full-scale values.

The hydrodynamic loads and their x-direction locations locating their effect on the shaft-bearing system are shown for both the ATD HPOTP and HPFTP two-bearing models in the Appendices of this report. These loads which represent the radial hydrodynamic effect of the major components of the HPOTP and HPFTP on the shaft are represented by concentrated force vectors. The force vectors that are in a three dimensional space were resolved into a x-y and x-z plane component form for entry into the SHABERTH input file. Also, in the Appendices are two tables from Pratt and Whitney [10] predicting the hydrodynamic radial effects and bearing reaction forces for 65%, 90% and 109% power levels. For each table, an angle orientation based on LH2 and LOX inlet and outlet ducts are shown. This angular orientation is also shown schematically in the load x-location diagrams for the 109% power level that are also located in the Appendices.

The axial preload that was placed arbitrarily on the shaft as a thrust load, is caused by the preload spring force axially loading the ball bearings in both turbopumps. For the ATD HPOTP, an axial preload of 1000 lb (4448 N) is imposed; whereas, for the ATD HPFTP, an axial preload of 650 lb. (2891 N) is imposed. This effect has been placed arbitrarily at the shaft's left end in the schematic loads diagrams in the Appendices. In the input file, the axial preload force was placed between the ball and roller bearings directed toward the pump-end ball bearing.

All of the inputs discussed can be found in the report's Appendices in correctly formatted locations. In the Appendices, an example input listing for the ATD HPOTP and HPFTP two-bearing model is presented. For each bearing, the bearing geometry is listed. Then, the initial steady-state temperatures for each bearing are listed at 13 locations on the bearing. These locations are explained in reference [5]. Next, the shaft dimensions and x-locations are presented and finally, the x-direction locations, with their corresponding radial loads and axial preload along with the x-direction bearing locations for both the x-y and x-z planes are presented.

At the end of each input file, SRS Technologies has added character strings to provide the user with options. The first option is the usage of a subroutine to calculate axial preload conditions for the bearings. The procedure to use the option is outlined in reference [9]. In this simulation, this option was not used. The axial preload for the HPOTP and HPFTP was manually placed into the load portion of the input file. The next option is the usage of SHABERTH only or the SHABERTH/SINDA iteration scheme. SINDA is a finite difference equation solver which uses the frictional heat generation output from SHABERTH based on the input initial temperatures and calculates a temperature field at predetermined points of the bearing. The results of the SINDA localized at the 13 temperature nodes on the bearing are substituted atop the original temperatures in SHABERTH until a 2°C thermal convergence occurs. At this time, SINDA models for the ATD ball and roller bearings do not exist. SRS Technologies is beginning work on a grid generation program to subdivide the nodal areas automatically. This program should expediate the process of inputting the nodal information and conductances into a SINDA input file which is a long and laborous task. Also, information concerning the coolant's flowrate and fluid properties must be added to the SHABERTH input file. These properties can be found in references [6,7] for LOX and LH2. For this project, only the SHABERTH program was used to model the turbopumps.

## RESULTS

Due to the length of time necessary to obtain the data and to construct the SHABERTH input files, an extensive parametric study was not feasible. The HPOTP and HPFTP case presented are only at the 109% and 65% power levels. At the 109% power level, the HPOTP shaft speed is 25,977 rpm while the HPFTP shaft speed is around 38,482 rpm. At the 65% power level, it's predicted that the HPOTP shaft speed is 17,000 rpm, whereas, the HPFTP shaft speed is 28,507 rpm.

Table 1 results show bearing reaction forces required to support the hydrodynamic radial loads and axial preloads that exist in both turbopumps. In Tables 1a and 1b, a comparison is made between the two-bearing SHABERTH model and Pratt and Whitney bearing reaction forces for the HPOTP. Pratt and Whitney's results are based on calculations using their predicted hydrodynamic radial loads. Table 1a and 1b results show close agreement in bearing reaction loads. A similar comparison can be made in Tables 1c and 1d for the HPFTP two bearing model reaction loads and the Pratt and Whitney results.

Even though there is good agreement in bearing reaction loads, no agreement could be found between the two bearing model and Pratt and Whitney's one bearing SHABERTH model for frictional heat generation. For the roller bearing under a 500 lb. radial load, Pratt and Whitney predicts the HPOTP frictional rates to be 191 W (watts) at 15,000 rpm and 320 W at 25,000 rpm. For their HPFTP model which reacts to a 2000 lb. radial load, their one bearing SHABERTH model predicts 923 W at 30,000 rpm and 1100 W at 35,000 rpm. In Tables 2a and 2b, the two bearing model results are compared to a one bearing model generated by the author to attempt an explanation for the discrepancy between Pratt and Whitney and the author's results. As shown in Tables 2a and 2b for the HPOTP at two different power levels, the ball bearing heat generation results closely agree for the one and two bearing models. However, the roller bearing heat generation rates are not as close numerically, but are similar in magnitude. However, neither of these models agree with Pratt and Whitney results. In Tables 2c and 2d for the HPFTP model, again, the ball bearing heat generation rates are comparable, however, the roller bearing rates are quite different. It seems that the one-bearing model underpredicts the two-bearing model by about one-half. This discrepancy may be explained due to a convergence error message that occurred in the one-bearing model. The default 15 iterations were not adequate for the solution subroutine. So, the results for my one-bearing model may not have totally converged. Again, neither of the models' results were comparable to Pratt and Whitney's one bearing model.

Finally, Table 3 shows the maximum contact Hertzian stresses for the inner and outer races for the HPOTP and HPFTP one and two bearing models. For the HPOTP one and two bearing model, Tables 3a and 3b show a good comparison of Hertz stress for the ball bearing; however, the roller bearing results are not as close numerically, but are the same order or magnitude. Tables 3c and 3d show a similar pattern for the HPFTP one and two bearing models. No results were obtained from Pratt and Whitney regarding Hertz stress. They use the A.B. Jones bearing program to calculate contact

stresses. In the initial design, a contact stress of around 300,000 psi (2068.4 MPa) is predicted to exist in the roller bearings. Again, my results tend to underpredict this value.

At this time, the cause for the agreement in reaction loads, but the discrepancies in frictional heat rates and Hertz stresses between Pratt and Whitney's results and the author's results are not known. The author recommends further effort be expended to verify the similarity of input data between the two bearing model and Pratt and Whitney models. More documentation of Pratt and Whitney's input and output for their SHABERTH and A.B. Jones models would be helpful to perform a better verification of results. If the comparison of inputs is exact, then, the author recommends the possibility of subtle differences that could exist between Pratt and Whitney's and NASA/MSFC SHABERTH programs.

Table 1a: HPOTP Bearing Reaction Loads  
 Axial Preload: 4483N (1000 lb)  
 109% power - (25,977 rpm)

Two Bearing Model					Pratt & Whitney Results		
	$F_X$	$F_Y$	$F_Z$	$F_R$	Angle	$F_R$	Angle
	(N)	(N)	(N)	(N) (lb)	(degrees)	(lb)	(degrees)
Ball Brg.	-4375	-667	-580	883.9 (198.7)	221	195	229
Roller Brg.	0	1640	-341	1675.1 (376.6)	101.7	375	102

Table 1b: HPOTP Bearing Reaction Loads  
 Axial Preload: 4483N (1000 lb)  
 65% power - (17,000 rpm)

Two Bearing Model					Pratt & Whitney Results		
	F <sub>X</sub>	F <sub>Y</sub>	F <sub>Z</sub>	F <sub>R</sub>	Angle		
	(N)	(N)	(N)	(N)	(degrees)		
				(lb)			
Ball Brg.	-4400	90.3	-177	198.7 (44.67)	152.9	45	152
Roller Brg.	0	1331	25.1	1331.2 (299.3)	88.92	300	90

Table 1c: HPFTP Bearing Reaction Loads  
 Axial Preload: 2891N (650 lb)  
 109% power - (38,482 rpm)

	Two Bearing Model					Pratt & Whitney Results	
	$F_X$ (N)	$F_Y$ (N)	$F_Z$ (N)	$F_R$ (N) (lb)	Angle (degrees)	$F_R$ (lb)	Angle (degrees)
Ball Brg.	-2797	-1242	473	132.9 (298.8)	20.8	300	25
Roller Brg.	0	9902	2349	10,176.8 (2287.8)	166.6	2275	167

Table 1d: HPFTP Bearing Reaction Loads  
 Axial Preload: 2891N (650 lb)  
 65% power - (28,507 rpm)

	Two Bearing Model					Pratt & Whitney Results	
	$F_X$ (N)	$F_Y$ (N)	$F_Z$ (N)	$F_R$ (N) (lb)	Angle (degrees)	$F_R$ (lb)	Angle (degrees)
Ball Brg.	-2831	-952	287	994.3 (223.5)	16.78	225	20
Roller Brg.	0	7262	1419	7399.3 (1663.5)	168.9	1660	169

Table 2a: HPOTP Frictional Heat Generation Rates (Watts)  
 109% power level (25,977 rpm)  
 (cage heat neglected)

	Two Bearing Model			One Bearing Model		
	Inner Race	Outer Race	Total	Inner Race	Outer Race	Total
Ball Brg.	2535	2477	5012	2564	2328	4892
Roller Brg.	17.5	25.1	42.6	12.3	20.3	32.5

Table 2b: HPOTP Frictional Heat Generation Rates (Watts)  
 65% power level (17,000 rpm)  
 (cage heat neglected)

	Two Bearing Model			One Bearing Model		
	Inner Race	Outer Race	Total	Inner Race	Outer Race	Total
Ball Brg.	1321	694	2015	1340	656	1996
Roller Brg.	12.1	13.7	25.8	9.66	11.5	21.16



Table 2c: HPFTP Frictional Heat Generation Rates (Watts)  
 109% power level (38,482 rpm)  
 (cage heat neglected)

	Two Bearing Model			One Bearing Model		
	Inner Race	Outer Race	Total	Inner Race	Outer Race	Total
Ball Brg.	2499	9515	12,014	2585	8766	11,351
Roller Brg.	98.6	163	261.6	36.9	85.3	122.2

Table 2d: HPFTP Frictional Heat Generation Rates (Watts)  
 65% power level (28,507 rpm)  
 (cage heat neglected)

	Two Bearing Model			One Bearing Model		
	Inner Race	Outer Race	Total	Inner Race	Outer Race	Total
Ball Brg.	1732	2821	4553	1793	2653	4446
Roller Brg.	77.2	97.1	174.3	34.7	51.4	86.1

Table 3a: HPOTP Maximum Hertzian Contact Stresses ( $\text{N/mm}^2$ )  
109% power level (25,977 rpm)

	Two Bearing Model		One Bearing Model	
	Inner Race	Outer Race	Inner Race	Outer Race
Ball Brg.	1989.2	1649.7	1990.3	1643.2
Roller Brg.	1433.5	1440.7	1250.9	1308.6

Table 3b: HPOTP Maximum Hertzian Contact Stresses ( $\text{N/mm}^2$ )  
65% power level (17,000 rpm)

	Two Bearing Model		One Bearing Model	
	Inner Race	Outer Race	Inner Race	Outer Race
Ball Brg.	1947.3	1412.4	1913.9	1398.5
Roller Brg.	1459.7	1358.8	1322.6	1237.3

Table 3c: HPFTP Maximum Hertzian Contact Stresses ( $\text{N/mm}^2$ )  
109% power level (38,482 rpm)

	Two Bearing Model		One Bearing Model	
	Inner Race	Outer Race	Inner Race	Outer Race
Ball Brg.	1806.5	1955.3	1946.2	1955.9
Roller Brg.	2192.2	2136.2	1605.3	1754.9

Table 3d: HPFTP Maximum Hertzian Contact Stresses ( $\text{N/mm}^2$ )  
65% power level (28,507 rpm)

	Two Bearing Model		One Bearing Model	
	Inner Race	Outer Race	Inner Race	Outer Race
Ball Brg.	1776.6	1660.7	1853.8	1667.5
Roller Brg.	2168.8	2008.3	1669.7	1635.5

### CONCLUSIONS AND RECOMMENDATIONS

Based on my limited results, no relationship can be established at this time concerning close agreement in the bearing loads; but, discrepancies in the bearing frictional heat rates and Hertz stresses between the author's and Pratt and Whitney's models. In a brief parametric study, it was found that frictional heat generation seemed to be sensitive to changes in diametrical clearance of the bearing, the dry coefficient of friction and the rotational speed of the shaft or bearing inner ring. Hertz stress seemed to be sensitive to the loading applied to the shaft-bearing system. The discrepancies between my one and two bearing models exist due to a convergence problem in the one bearing model solution scheme. The error warnings allowed for calculations to be executed; however, suggested that these calculations may not be totally converged to the 0.01 limit within 15 iterations.

Based on this study, several recommendations for future research in this are as follows.

1. Further efforts are needed to establish commonality in the input parameters between Pratt and Whitney and the independent SHABERTH user. This is especially important when the design process dictates changes in the ATD HPOTP and HPFTP bearing configurations.
2. The establishment of SINDA models are needed for HPOTP and HPFTP roller and ball bearing. This will allow a possible thermally converged solution to occur as a result of the SHABERTH/SINDA iteration scheme.
3. The parametric investigation concerning the sensitivity of bearing parameter inputs based on their effect to selected SHABERTH outputs as bearing frictional heat generation, Hertz stress, clearances and bearing reaction forces should be performed.

Hopefully, from these recommendations, a useful numerical model of the ATD HPOTP and ATD HPFTP can be constructed. These models could become an important independent source of information when comparing its results to bearing tester data on the eventual ATD turbopump test data. Also, parametric studies using these models can provide a relatively economical means to predict possible problem areas in bearing performances. However, for SHABERTH's results to be a reliable predictor of bearing

performances, it must have reliable inputs based upon both experimental data and analytical formulation. As the ATD develops from the design and development stages into the construction and testing stages, SHABERTH coupled with SINDA can become an important evaluation tool for the bearing performance when subjected to the various power levels experienced in flight.

ORIGINAL PAGE IS  
OF POOR QUALITY

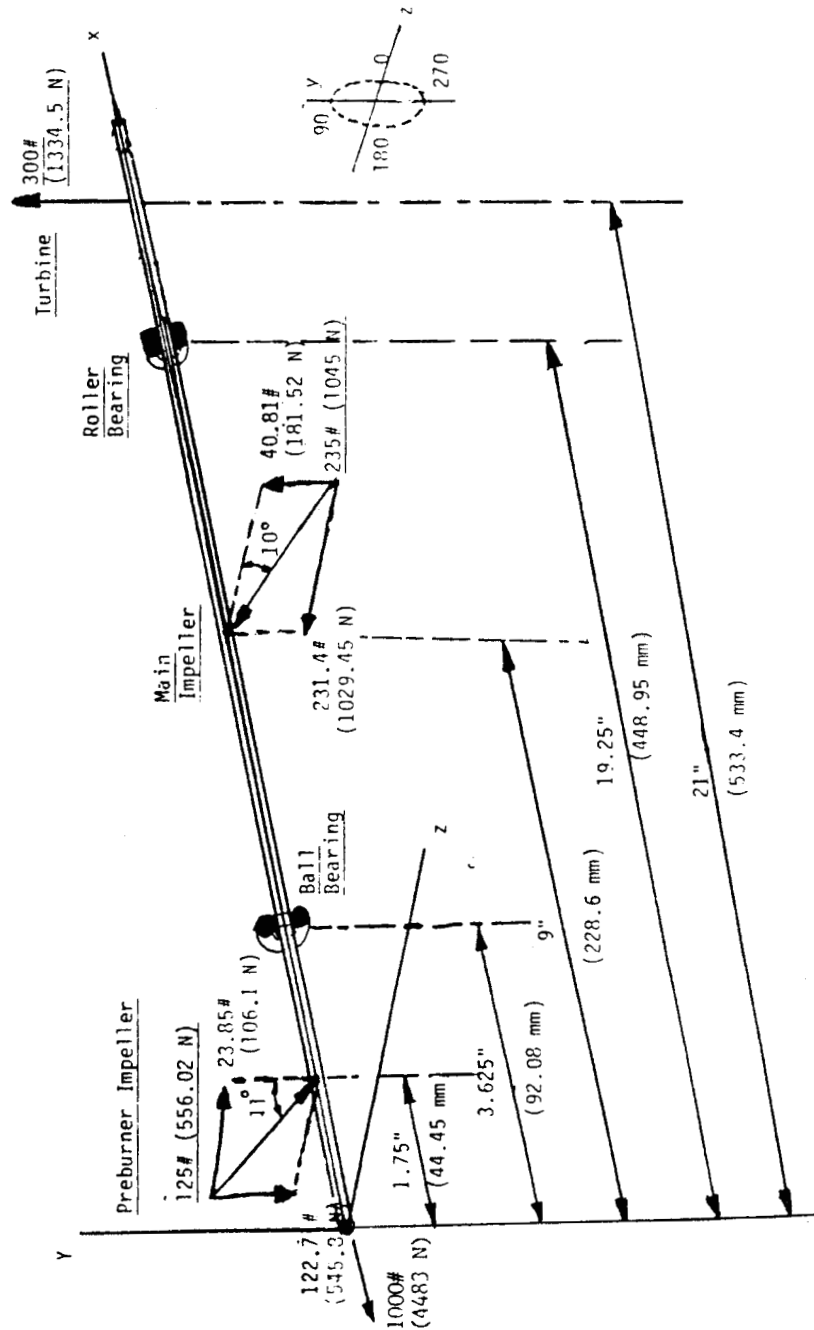
REFERENCES

1. Harris, Tedric A., Roller Bearing Analysis, 2nd edition. A Wiley-Interscience Publication of John Wiley and Sons, New York, NY, 1984.
2. Eschmann, Hasbargen, and Weigand, Ball and Roller Bearings; Theory, Design and Application. John Wiley and Sons, New York, NY, 1985.
3. Palmgren, Arvid, Ball and Roller Bearing Engineering, 3rd edition. SKF Industries, Inc., Philadelphia, PA, 1959.
4. Crecelius, W.J. and J. Pirvics, Computer Program Operation Manual on SHABERTH Computer Program for the Analysis of the Steady State and Transient Thermal Performance of the Shaft-Bearing Systems. Technical Report AFAPL-TR-76-90 (SKF report AL76PO30), Air Force Aero Propulsion Laboratory and Naval Air Propulsion Test Center, October, 1976.
5. Hadden, G.B., R.J. Kleckner, M.A. Ragen, L. Sheynin, Research Report-User's Manual for the Computer Program AT81Y003 SHABERTH (Steady-State, Transient Thermal, Ball, Cylindrical and Tapered Roller Bearings), SKF Report No. AT81D040, submitted to NASA-Lewis, Cleveland, OH under contract NAS3-22690, COSMIC program #LEW-12761, May 1981.
6. McCarty, R.D. and L.A. Weber, Thermophysical Properties of Oxygen from Freezing Liquid Line to 600°R for Pressures to 5000 psia. NBS-TN-384, U.S. Department of Commerce, National Bureau of Standards, July 1971.
7. McCarty, R.D. and L.A. Weber, Thermophysical Properties of Parahydrogen from the Freezing Liquid Line to 5000°R for Pressures to 10,000 psia, NBS-TN-617, U.S. Department of Commerce, National Bureau of Standards, April 1972.
8. SSME Alternate Turbopump Development Program Design Review Package (prepared under NASA contract NAS8-36801 for NASA/MSFC by Pratt and Whitney), FR-19821-1, May 16, 1987.

9. "User's Guide for the Mechanical/Thermal Model for the HPOTP Pump-end Bearings," SRS-Technologies, System Technology Division, Huntsville, AL, (not dated--written by D. Marty).
10. "SSME/ATD Side Load and Resultant Bearing Loads in Support of NASA Rid No. 109," memo from David B. Hudson to John L. Price, Pratt and Whitney Government Product Division Internal Correspondence, 88167E010047, June 15, 1988.

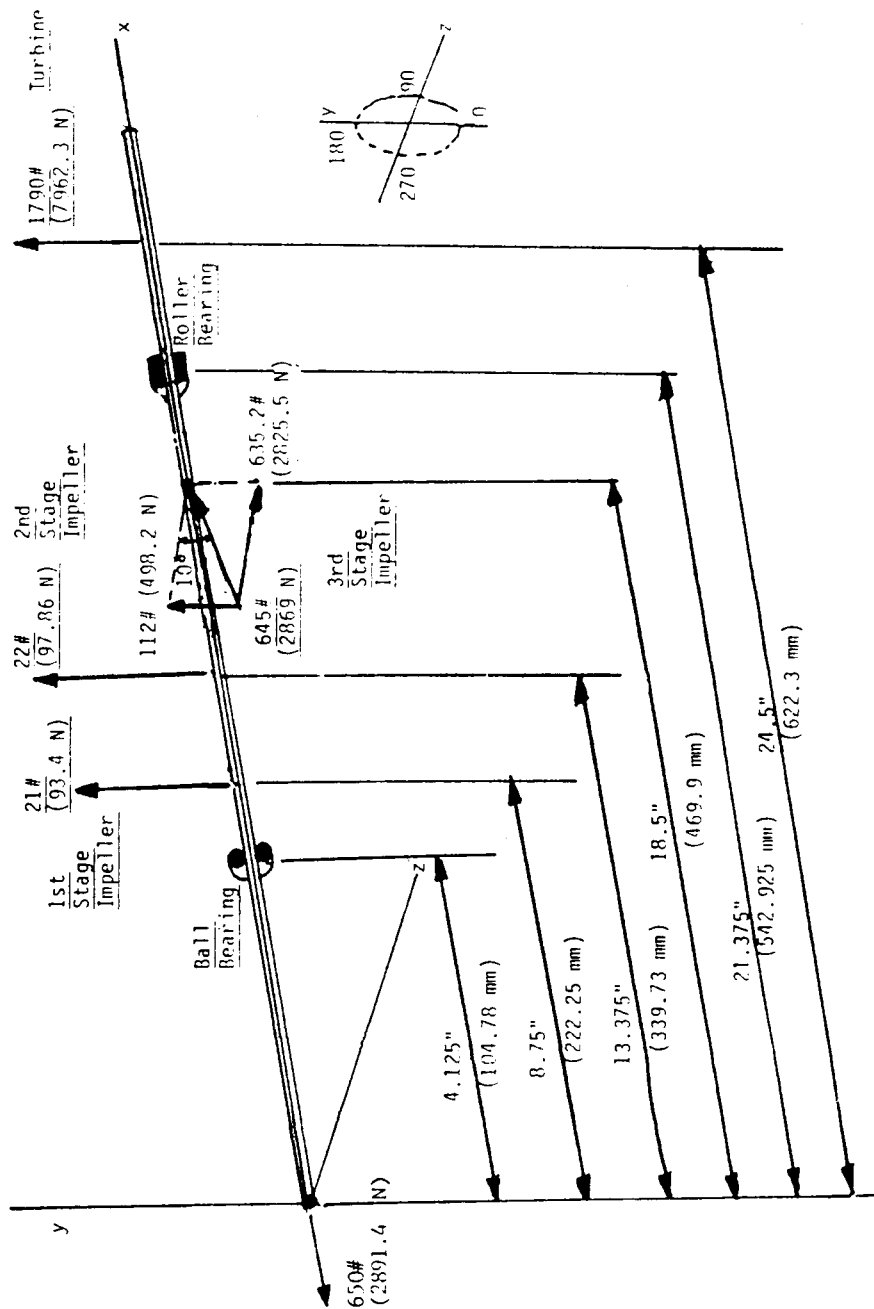
APPENDICES

Schematic of HPOTP Hydrodynamic Loads





# Schematic of HPFTP Hydrodynamic Loads



ORIGINAL PAGE IS  
OF POOR QUALITY

ORIGINAL PAGE IS  
OF POOR QUALITY

HPOTP Hydrodynamic Radial Loads [10]

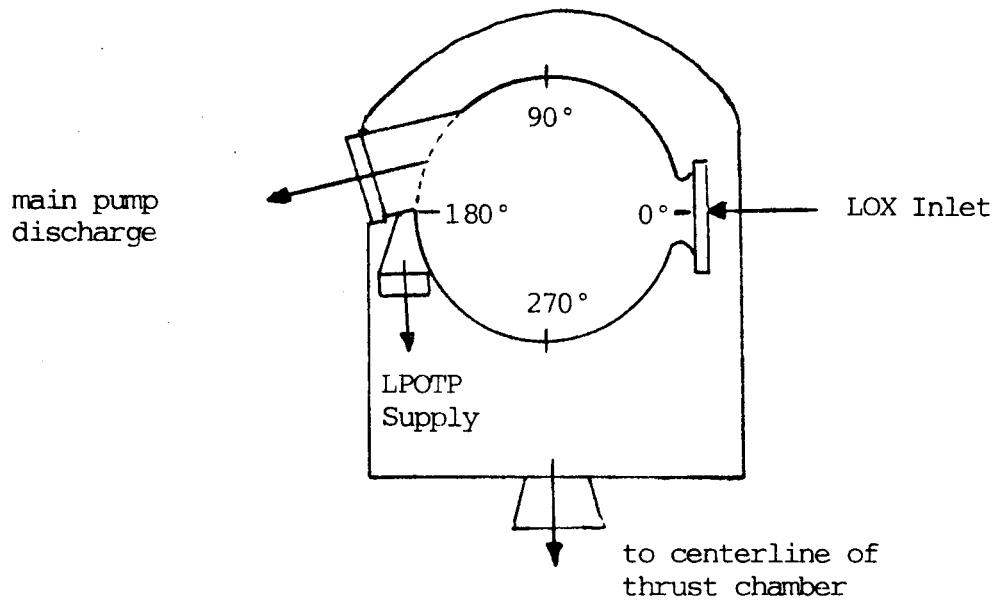
Device	Power Level					
	65%		90%		109%	
	Load (lb)	Angle (degree)	Load (lb)	Angle (degree)	Load (lb)	Angle (degree)
Preburner Impeller	87	67	106	84	125	101
Main-Stage Impeller	200	270	220	310	235	350
Turbine	200	270	260	270	300	270
Resultant Bearing Loads (lb)						
Ball Brg (pump-end)	45	152	115	160	195	229
Roller Brg. (turbine end)	300	90	365	97	375	102

HPFTP Hydrodynamic Radial Loads [10]

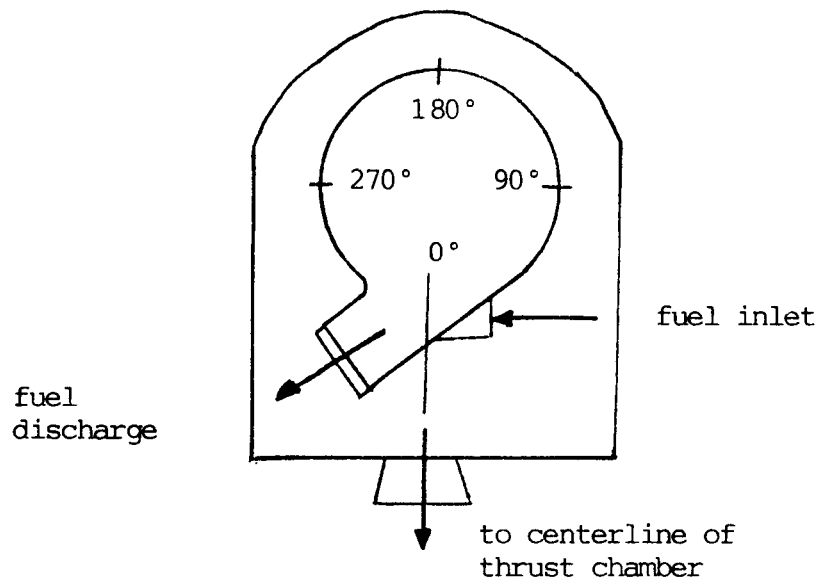
Device	Power Level					
	65%		90%		109%	
	Load (lb)	Angle (degree)	Load (lb)	Angle (degree)	Load (lb)	Angle (degree)
1st Stage Impeller	12	0	17	0	21	0
2nd Stage Impeller	13	0	18	0	22	0
3rd Stage Impeller	390	280	530	280	645	280
Turbine	1325	0	1580	0	1790	0
Resultant Brg. Loads (lb)						
Ball Brg. (pump end)	225	20	265	23	300	25
Roller Brg. (turbine end)	1660	169	2000	168	2275	167

ORIGINAL PAGE IS  
OF POOR QUALITY

HPOTP (from pump-end looking toward turbine-end)



HPFTP (from pump-end looking toward turbine-end)



# HPOTP Two-Bearing SHABERTH Input

SSME (P&W-ATD) LOX TURBOPUMP (ATD-HPOTP) -- BALL & ROLLER BEARINGS- 109%

25977. 2 0 5 -20 .001 .010 11

B1 440C 440C 3. 3. 0.

95.000 11 .1696 3.67 0

20.6000

.52 .58

.014 .014 .014 2. 2. 2.

+1 84.176 3.99 0.254 0.43 .136 3

.058420 -.11680 34.96 34.96 30.60 30.60

20.00 60.00 80.88 109.70 130.00 181.0

2.065E5 2.090E5 2.090E5 2.050E5 2.065E5

.279 .270 .270 .270 .275

8.210 7.740 7.740 7.740 8.210

11.16E-6 9.346E-6 9.346E-6 9.346E-6 10.980E-6

.0.250 .0.200

C2 440C (AMS 5618) AMS 6265 (AISI 9310) 1. 1. 0.

100.000 14 -.0381 0

15.000 15.000 695.96 7.62

15.000 15.000 20.

0.000 0.250 1.041 10.

0.200 0.200 0.20 1.500 1.50 1.50

0.200 0.200 0.20 1.500 1.50 1.50

-1.0 91.14 6.29 0.546 0.445 .1295

0.0508 -0.1168 28.64 28.64 30.54 30.54

20.00 73.0 85.0 115.0 127.0 178.0

2.188E5 2.120E5 2.120E5 2.180E5 2.231E5

0.294 0.262 0.262 0.296 0.280

8.220 7.250 7.250 8.190 7.750

10.850E-6 7.257E-6 7.257E-6 8.076E-6 12.522E-6

.0.100 .0.100

0.1

-145.-145.-145.-145.-145.-145.-145.-145.-145.-145.-145.-145.

-118.-118.-118.-118.-118.-118.-118.-118.-118.-118.-118.-118.

1 0.0 0.0 11.67 0.0 33.34 2.121E5

1 63.50 11.67 23.34 33.34 33.34 2.121E5

1 69.85 23.34 23.34 33.34 40.01 2.121E5

1 76.20 23.34 20.00 40.01 60.01 2.121E5

1 107.95 20.00 20.00 60.01 40.04 2.121E5

1 228.60 20.00 20.00 40.04 48.34 2.121E5

1 406.40 20.00 20.00 48.34 60.01 2.121E5

1 444.50 20.00 20.00 60.01 73.34 2.121E5

1 555.63 20.00 0.0 73.34 0.0 2.121E5

2 92.08 0.0 0.0

2 488.95 0.0 0.0

3 44.45 -545.8 0.0 0.0 0.0 0.0

3 228.60 181.5 0.0 0.0 0.0 -4448.

3 533.40 1334.5 0.0 0.0 0.0 0.

2 1 0.0 0.0

2 2 0.0 0.0

3 44.45 106.1 0.0 0.0 0.0 0.

3 228.60 -1029.5 0.0 0.0 0.0 0.

3

SBRGNUM

LOUT=1

SEND

SJSPRG

PREDEF=1.36839E-2,KSPRNG=82000., PLOAD=478.60, DELMX=15.5E-3,

INTCL=.0063, TCRUV=.06125

SEND

SFLGS

FLAG='NOSPRG', SFLAG='SHA', AXLOAD= .TRUE.,.TRUE.,.TRUE.,.TRUE.

SEND

Ball  
Bearing

Roller  
Bearing

Initial  
Temperatures

Shaft  
Dimensions

Radial &  
Axial Loads  
(x-y plane)

Radial Loads  
(x-z plane)

SSME (P&amp;W-ATD) LH2 TURBOPUMP (ATD-HPFTP) -- BALL &amp; ROLLER BEARINGS- 109°

38482.	2	0	5	-20	.001	.010	11
B1	440C		440C		3.	3.	0.
95.000		11	.1696	3.67		0	
20.6000							
.52	.58						
.014	.014	.014	2.	2.	2.		
+1	84.176	3.99	0.254	0.43	.136	3	
.058420	-.11680	34.96	34.96	30.60	30.60		
20.00	60.00	80.88	109.70	130.00	181.0		
2.065E5	2.090E5	2.090E5	2.050E5	2.065E5			<u>Ball</u>
.279	.270	.270	.270	.275			<u>Bearing</u>
8.210	7.740	7.740	7.740	8.210			
11.16E-6	9.346E-6	9.346E-6	9.346E-6	10.980E-6			
			0.250	0.200			
C2	440C(AMS 5618)	AMS 6265(AISI 9310)	1.	1.	0.		
103.000	14	-.0635		0			
17.000	17.000		632.50	8.89			
17.000	17.000				20.		
0.000	0.250		1.245	10.			
0.200	0.200	0.20	1.500	1.50	1.50		
0.200	0.200	0.20	1.500	1.50	1.50		<u>Roller</u>
-1.0	93.00	5.81	0.546	0.445	.1810		<u>Bearing</u>
0.1270	-0.1980	34.61	34.61	32.54	32.54		
20.00	73.0	86.0	120.0	133.0	178.0		
2.188E5	2.120E5	2.120E5	2.180E5	2.231E5			
0.294	0.262	0.262	0.296	0.280			
8.220	7.250	7.250	8.190	7.750			
10.850E-6	7.257E-6	7.257E-6	8.076E-6	12.522E-6			
			0.100	0.100			0.10
			1				
-202.-202.-202.-202.-202.-202.-202.-202.-202.-202.-202.-202.							<u>Initial</u>
-202.-202.-202.-202.-202.-202.-202.-202.-202.-202.-202.-202.							<u>Temperatures</u>
1	0.0	0.0	20.00	0.0	41.67	2.121E5	
1	69.85	20.00	20.00	41.67	60.00	2.121E5	
1	120.65	20.00	20.00	60.00	41.67	2.121E5	
1	198.40	20.00	20.00	41.67	48.30	2.121E5	
1	312.70	20.00	20.00	48.30	51.67	2.121E5	<u>Shaft</u>
1	436.60	20.00	20.00	51.67	58.34	2.121E5	<u>Dimensions</u>
1	501.65	20.00	20.00	58.34	63.34	2.121E5	
1	519.11	20.00	20.00	63.34	73.34	2.121E5	
1	657.23	20.00	0.0	73.34	0.0	2.121E5	
2	104.78	0.0		0.0			
2	542.93	0.0		0.0			
3	222.25	93.4	0.0	0.0	0.0	-2891.3	<u>Radial &amp;</u>
3	339.73	97.9	0.0	0.0	0.0	0.	<u>Axial Loads</u>
3	469.90	498.2	0.0	0.0	0.0	0.	<u>(x-y plane)</u>
3	622.30	7962.3	0.0	0.0	0.0	0.	
2	1	0.0		0.0			
2	2	0.0		0.0			
3	469.90	2825.5	0.0	0.0	0.0	0.	<u>Radial Load</u>
							<u>(x-z plane)</u>
3							

SBRGNUM

LOUT=1

SEND

SJSPRG

PREDEF=1.36839E-2,KSPRNG=82000., PLOAD=478.60, DELMX=15.5E-3,  
INTCL=.0063, TCRUV=.06125

SEND

SFLGS

FLAG='NOSPRG',SFLAG='SHA', AXLOAD= .TRUE.,.TRUE.,.TRUE.,.TRUE.

SEND

# HPOTP One-Bearing SHABERTH Input (Ball Bearing)

```

SSME (P&W-ATD) LOX TURBOPUMP (ATD-HPOTP) - SINGLE BALL BEARING - 109%
25977. 1 1 1
B1 440C 440C 1. 1. 0.
95.000 11 .1696 3.67 0.
20.6
0.52 0.58
0.014 0.014 0.014 2.0 2.0 2.0
-1.0 84.18 3.99 0.254 0.432 .1360
0.250 0.200
-145.-145.-145.-145.-145.-145.-145.-145.-145.-145.-145.-145.
883.9 Radial Load -4448. Axial Load
Ball
Bearing
Initial
Temperatures

SERGNUM
LOUT=1
SEND
SJSPRG
PREDEF=1.36839E-2,KSPRNG=82000., PLOAD=478.60, DELMX=15.5E-3,
INTCL=.0063, TCRUV=.06125
SEND
SFLGS
FLAG='NOSPRG',SFLAG='SHA', AXLOAD=.TRUE.,.TRUE.,.TRUE.,.TRUE.
SEND

```

# HPOTP One-Bearing SHABERTH Input (Roller Bearing)

```

SSME (P&W-ATD) LOX TURBOPUMP (ATD-HPOTP) -- SINGLE ROLLER BEARING - 109%
25977. 1 1 1
C1 440C(AHS 5618) AMS 6265(AISI 9310) 1. 1. 0.
100.000 14 -.0381 0.
15.000 15.000 695.96 7.62
15.000 15.000 20.
0.000 0.250 1.041 10.
0.200 0.200 0.20 1.500 1.50 1.50
0.200 0.200 0.20 1.500 1.50 1.50
-1.0 91.14 6.30 0.546 0.445 .1295
0.100 0.100 0.10
-118.-118.-118.-118.-118.-118.-118.-118.-118.-118.-118.-118.
1675.1 Radial Load
Roller
Bearing
Initial
Temperatures

SBRGNUM
LOUT=1
SEND
SJSPRG
PREDEF=1.36839E-2,KSPRNG=82000., PLOAD=478.60, DELMX=15.5E-3,
INTCL=.0063, TCRUV=.06125
SEND
SFLGS
FLAG='NOSPRG',SFLAG='SHA', AXLOAD=.TRUE.,.TRUE.,.TRUE.,.TRUE.
SEND

```

ORIGINAL PAGE IS  
OF POOR QUALITY

HPFTP One-Bearing SHABERTH Input  
(Ball Bearing)

```

SSME (P&W-ATD) LH2 TURBOPUMP (ATD-HPFTP) - SINGLE BALL BEARING - 109%
38482. 1 1 1
B1 440C 440C 1. 1. 0.
95.000 11 .1696 3.67 0.
20.6
0.52 0.58
0.014 0.014 0.014 2.0 2.0 2.0
-1.0 84.18 3.99 0.254 0.432 .1360
0.250 0.200
1
-202.-202.-202.-202.-202.-202.-202.-202.-202.-202.-202.-202.
1329.0 Radial Load -2891.3 Axial Load Initial
Temperatures

SBRGNUM
LOUT=1
SEND
SJSPRG
PREDEF=1.36839E-2,KSPRNG=82000., PLOAD=478.60, DELMX=15.5E-3,
INTCL=.0063, TCRUV=.06125
SEND
$FLGS
FLAG='NOSPRG' ,SFLAG='SHA', AXLOAD= .TRUE.,.TRUE.,.TRUE.,.TRUE.
SEND

```

HPFTP One-Bearing SHABERTH Input  
(Roller Bearing)

```

SSME (P&W-ATD) LH2 TURBOPUMP (ATD-HPFTP) -- SINGLE ROLLER BEARING - 109%
38482. 1 1 1
C1 440C(AMS 5618) AMS 6265(AISI 9310) 1. 1. 0.
103.000 14 -.0635 0.
17.000 17.000 632.50 8.89
17.000 17.000 20.
0.000 0.250 1.245 10.
0.200 0.200 0.20 1.500 1.50 1.50
0.200 0.200 0.20 1.500 1.50 1.50
-1.0 93.00 5.81 0.546 0.445 .1810
0.100 0.100 0.10
1
-202.-202.-202.-202.-202.-202.-202.-202.-202.-202.-202.-202.
10176.8 Radial Load Initial
Temperatures

SBRGNUM
LOUT=1
SEND
SJSPRG
PREDEF=1.36839E-2,KSPRNG=82000., PLOAD=478.60, DELMX=15.5E-3,
INTCL=.0063, TCRUV=.06125
SEND
$FLGS
FLAG='NOSPRG' ,SFLAG='SHA', AXLOAD= .TRUE.,.TRUE.,.TRUE.,.TRUE.
SEND

```